



Contents lists available at ScienceDirect

## Marine Micropaleontology

journal homepage: [www.elsevier.com/locate/marmicro](http://www.elsevier.com/locate/marmicro)

Research paper

Modelling  $\delta^{13}\text{C}$  in benthic foraminifera: Insights from model sensitivity experimentsT. Hesse <sup>a,\*</sup>, D. Wolf-Gladrow <sup>a</sup>, G. Lohmann <sup>a</sup>, J. Bijma <sup>a</sup>, A. Mackensen <sup>a</sup>, R.E. Zeebe <sup>b</sup><sup>a</sup> Alfred Wegener Institute for Polar and Marine Research, D-27570 Bremerhaven, Germany<sup>b</sup> School of Ocean and Earth Science and Technology, University of HI at Manoa, 1000 Pope Road, MSB 504, Honolulu 96822, USA

## ARTICLE INFO

## Article history:

Received 19 December 2012

Received in revised form 9 July 2014

Accepted 7 August 2014

Available online 16 August 2014

## Keywords:

Carbon isotopes

Vital effect

Carbonate ion effect

Palaeoceanography

Last Glacial Maximum

Phytodetritus

## ABSTRACT

The  $\delta^{13}\text{C}$  value measured on benthic foraminiferal tests is widely used by palaeoceanographers to reconstruct the distribution of past water masses. The biogeochemical processes involved in forming the benthic foraminiferal  $\delta^{13}\text{C}$  signal ( $\delta^{13}\text{C}_{\text{foram}}$ ), however, are not fully understood and a sound mechanistic description is still lacking. We use a reaction–diffusion model for calcification developed by Wolf-Gladrow et al. (1999) and Zeebe et al. (1999) in order to quantify the effects of different physical, chemical, and biological processes on  $\delta^{13}\text{C}_{\text{foram}}$  of an idealised benthic foraminiferal shell.

Changes in the  $\delta^{13}\text{C}$  value of dissolved inorganic carbon ( $\delta^{13}\text{C}_{\text{DIC}}$ ) cause equal changes in  $\delta^{13}\text{C}_{\text{foram}}$  in the model. The results further indicate that temperature, respiration rate, and pH have a significant impact on  $\delta^{13}\text{C}_{\text{foram}}$ . In contrast, salinity, pressure, the  $\delta^{13}\text{C}$  value of particulate organic carbon ( $\delta^{13}\text{C}_{\text{POC}}$ ), total alkalinity, and calcification rate show only a limited influence. In sensitivity experiments we assess how combining these effects can influence  $\delta^{13}\text{C}_{\text{foram}}$ . We can potentially explain 33 to 47% of the interglacial-to-glacial decrease in  $\delta^{13}\text{C}_{\text{foram}}$  by changes in temperature and pH, without invoking changes in  $\delta^{13}\text{C}_{\text{DIC}}$ . Furthermore, about a quarter of the  $-0.4\text{‰}$  change in  $\delta^{13}\text{C}_{\text{foram}}$  observed in phytodetritus layers can be accounted for by an increase in respiration rate and a reduction in pH.

© 2014 Elsevier B.V. All rights reserved.

## 1. Introduction

Benthic foraminiferal shell  $\delta^{13}\text{C}$  values ( $\delta^{13}\text{C}_{\text{foram}}$ ) have been widely used as a proxy for reconstructing the distributions of past ocean water masses, particularly in the Atlantic Ocean (Curry et al., 1988; Duplessy et al., 1988; Sarnthein et al., 1994; Mackensen et al., 2001; Bickert and Mackensen, 2004; Curry and Oppo, 2005; Hesse et al., 2011). Implicit in these studies is the assumption that the  $\delta^{13}\text{C}_{\text{foram}}$  value records the dissolved inorganic carbon  $\delta^{13}\text{C}$  value ( $\delta^{13}\text{C}_{\text{DIC}}$ ) of the water mass in which the foraminifera grow. Foraminifera record  $\delta^{13}\text{C}_{\text{DIC}}$  as  $\delta^{13}\text{C}_{\text{foram}}$  with offsets depending on species and habitat. Infaunal species tend to record lower  $\delta^{13}\text{C}_{\text{foram}}$  values than epifaunal ones (e.g. Grossman (1987); McCorkle et al. (1990); Rathburn et al. (1996)). Therefore, many authors of palaeoceanographic studies have focused on epifaunal species such as *Cibicides wuellerstorfi* Schwager 1866, that record  $\delta^{13}\text{C}_{\text{DIC}}$  more faithfully in a 1:1 relationship (Woodruff et al., 1980; Zahn et al., 1986; Duplessy et al., 1988; Hodell et al., 2001). Another complication, however, is the fact that even these species record an offset in their  $\delta^{13}\text{C}_{\text{foram}}$  signal with respect to  $\delta^{13}\text{C}_{\text{DIC}}$  under certain conditions, such as in algal bloom-derived phytodetritus layers (Mackensen et al., 1993; Zarriss and Mackensen, 2011).

Unfortunately, not much is known about the biological life cycles and behaviour of deep-sea benthic foraminifera due to their difficult-to-reach habitats. In-situ measurements of respiration and calcification rates of deep-sea benthic foraminiferal species do, to the best of our knowledge, not exist. Some authors have measured these rates under laboratory conditions (e.g. Hannah et al. (1994); Nomaki et al. (2007); Geslin et al. (2011); Glas et al. (2012)). Since it is notoriously difficult to culture deep-sea benthic foraminifera in the laboratory under in-situ conditions, culture experiments are often limited to shallow-water species (Chandler et al., 1996), or specimen taken from water depths shallower than 250 m (Wilson-Finelli et al., 1998; Havach et al., 2001). Culturing systems like those developed by Hintz et al. (2004) have allowed for systematic experiments on deep sea benthic foraminifera (Nomaki et al., 2005, 2006; McCorkle et al., 2008; Barras et al., 2010; Filipsson et al., 2010). From a theoretical point of view, progress has mostly been made on planktonic foraminifera (Wolf-Gladrow et al., 1999; Zeebe et al., 1999). In the benthic realm the impact of porewater on the diffusive boundary layer above the sediment–water interface (thickness of about 1 mm according to Archer et al. (1989)) may need to be considered when interpreting  $\delta^{13}\text{C}_{\text{foram}}$  (Zeebe, 2007).

Understanding and quantifying the various influences on the composition of  $\delta^{13}\text{C}_{\text{foram}}$  values are of paramount importance for validating any reconstruction of past water masses based on the  $\delta^{13}\text{C}$  proxy.

\* Corresponding author at: Öko-Institut e.V., Merzhauser Str. 173, D-79100 Freiburg, Germany.

E-mail address: [tilman.hesse@awi.de](mailto:tilman.hesse@awi.de) (T. Hesse).

We assess the potential impact of different physical, biological and carbonate chemistry processes on benthic  $\delta^{13}\text{C}_{\text{foram}}$  values by making model sensitivity experiments. We highlight some uncertainties in

$\delta^{13}\text{C}_{\text{foram}}$  values and put upper limits on their extent. For that we employ an adapted version of a diffusion–reaction model developed by Wolf-Gladrow et al. (1999) and Zeebe et al. (1999).

## 2. Methods

### 2.1. General model description

The model is a reaction–diffusion model of the carbonate system in seawater around an idealised spherical foraminiferal shell (Wolf-Gladrow et al., 1999). Carbon isotopes have been included in the model by Zeebe et al. (1999), which allows for the simulation of the shell's final  $\delta^{13}\text{C}_{\text{foram}}$  value. Boundary conditions are set by the bulk seawater conditions far away from the shell (outer boundary condition set at a distance of ten times the shell radius), and by the rates of exchange across the simulated shell surface (inner boundary condition, see Fig. 1 for a schematic drawing of the model geometry). Bulk seawater properties used as model input are temperature, salinity, pressure, pH,  $\delta^{13}\text{C}_{\text{DIC}}$ ,  $\delta^{13}\text{C}_{\text{POC}}$  (the  $\delta^{13}\text{C}$  of particulate organic carbon, i.e. the foraminifer's food, which is important for respiration), and total alkalinity (TA). Foraminifer-specific model input includes respiration rate and calcification rate. Given these inputs, the model iteratively calculates the concentrations of  $\text{H}^+$ ,  $\text{OH}^-$ ,  $\text{CO}_2$ ,  $\text{HCO}_3^-$ ,  $\text{CO}_3^{2-}$ ,  $\text{B}(\text{OH})_3$  and  $\text{B}(\text{OH})_4^-$  as well as the  $\delta^{13}\text{C}$  values of the carbonate system species ( $\text{CO}_2$ ,  $\text{HCO}_3^-$ ,  $\text{CO}_3^{2-}$ ) with distance from the shell, and the final  $\delta^{13}\text{C}_{\text{foram}}$ . Concentration calculations are based on molecular diffusion, the reactions between the different carbonate system species, and sources or sinks for the different chemical species at the boundary of the modelled calcite shell (see Wolf-Gladrow et al. (1999) for details). The general form of the equations for the concentration  $c(r, t)$  of a carbonate system species is:

$$0 = \frac{\partial c(r, t)}{\partial t} = \text{Diffusion} + \text{Reaction} + \text{Uptake}, \quad (1)$$

where  $r$  is the distance from the centre of the shell and  $t$  is time. The full diffusion–reaction equations for total carbon ( $\text{C} = {}^{13}\text{C} + {}^{12}\text{C}$ ) can be found in Wolf-Gladrow et al. (1999). Here we only give the example for  $\text{CO}_2$  (the remaining equations can be found in Appendix A):

$$0 = \frac{D_{\text{CO}_2}}{r^2} \frac{d}{dr} \left( r^2 \frac{d[\text{CO}_2]}{dr} \right) + (k_{-1} [\text{H}^+] + k_{-4}) [\text{HCO}_3^-] - (k_{+1} + k_{+4} [\text{OH}^-]) [\text{CO}_2], \quad (2)$$

where  $D_{\text{CO}_2}$  is the diffusion coefficient of  $\text{CO}_2$  in seawater, and the reaction rate constants are  $k_i$ . The equivalent equation for  ${}^{13}\text{CO}_2$  reads (see also Appendix A):

$$0 = \frac{D_{{}^{13}\text{CO}_2}}{r^2} \frac{d}{dr} \left( r^2 \frac{d[{}^{13}\text{CO}_2]}{dr} \right) + (k'_{-1} [\text{H}^+] + k'_{-4}) [\text{H}^{13}\text{CO}_3^-] - (k'_{+1} + k'_{+4} [\text{OH}^-]) [{}^{13}\text{CO}_2]. \quad (3)$$

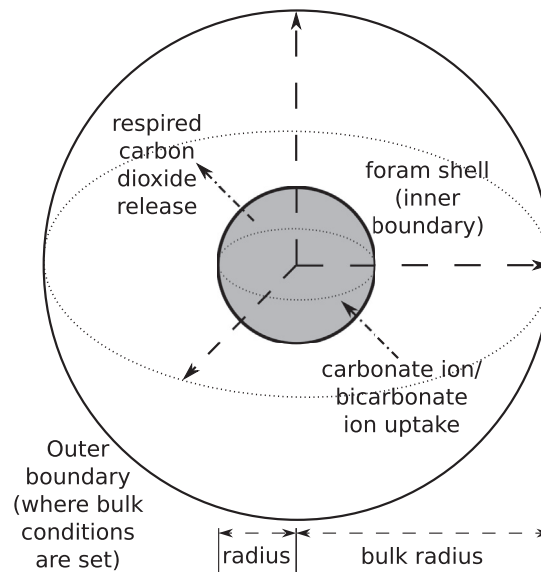


Fig. 1. Schematic representation of the foraminifer calcification model in spherical geometry.

The kinetic rate constants for  $^{13}\text{C}$  ( $k_i'$ ) are used to take into account kinetic fractionation effects (see Zeebe et al. (1999) for details). Temperature-dependent equilibrium fractionation between the various carbonate system species in bulk seawater is taken from Mook (1986) and Zeebe et al. (1999):

$$\begin{aligned}\varepsilon_1 &= \varepsilon_{(\text{CO}_{2(\text{g})} - \text{HCO}_3^-)} = -\frac{9483}{T} + 23.89 \\ \varepsilon_2 &= \varepsilon_{(\text{CO}_{2(\text{aq})} - \text{CO}_{2(\text{g})})} = -\frac{373}{T} + 0.19 \\ \varepsilon_3 &= \varepsilon_{(\text{CO}_{2(\text{aq})} - \text{HCO}_3^-)} = -\frac{9866}{T} + 24.12 \\ \varepsilon_4 &= \varepsilon_{(\text{CO}_3^{2-} - \text{HCO}_3^-)} = -\frac{867}{T} + 2.52 \\ \varepsilon_5 &= \varepsilon_{(\text{CaCO}_{3(\text{calc})} - \text{HCO}_3^-)} = -\frac{4232}{T} + 15.10 \\ \varepsilon_6 &= \varepsilon_{(\text{CaCO}_{3(\text{calc})} - \text{CO}_3^{2-})} = -\frac{3341}{T} + 12.54\end{aligned}\quad (4)$$

where  $T$  is absolute temperature in Kelvin. The model is capable of simulating both  $\text{HCO}_3^-$  uptake and  $\text{CO}_3^{2-}$  uptake.

We are using the model in order to make sensitivity simulations for deep-sea benthic foraminifera. Since the model has so far only been used for planktonic foraminifera living close to the sea surface, we introduced the dissociation constants' pressure dependence based on Millero (1995):

$$\ln\left(\frac{k_i^P}{k_i^0}\right) = -\left(\frac{\Delta V_i}{RT}\right)P + 0.5\left(\frac{\Delta \kappa_i}{RT}\right)P^2, \quad (5)$$

where  $k_i$  is the dissociation constant for reaction  $i$  between two carbonate system species,  $P$  the pressure in bars,  $R = 8.314 \text{ m}^3 \text{ Pa K}^{-1} \text{ mol}^{-1}$  the gas constant,  $T$  the temperature in Kelvin,  $\Delta V_i$  the associated molal volume change in ( $\text{m}^3 \text{ mol}^{-1}$ ), and  $\Delta \kappa_i$  the associated compressibility change in ( $\text{m}^3 \text{ Pa}^{-1} \text{ mol}^{-1}$ ). The latter two are calculated as follows:

$$\Delta V_i = a_0 + a_1 T_c + a_2 T_c^2 \quad (6)$$

and

$$\Delta \kappa_i = b_0 + b_1 T_c \quad (7)$$

where  $T_c$  is temperature in  $^\circ\text{C}$  and the coefficients are shown in Table 1. Additionally, we removed the original model's symbiotic algae component.

## 2.2. Model input parameters

First, we performed sensitivity simulations for different external bulk parameters. These parameters are  $\delta^{13}\text{C}_{\text{DIC}}$ , temperature, salinity, pressure,  $\delta^{13}\text{C}_{\text{POC}}$ , pH, and TA. Second, we varied parameters related to the foraminifer, i.e. respiration rate and calcification rate. When varying one parameter all other parameters were kept constant at generic deep-sea values (see Table 2).

There are only few measurements of vital rates in benthic foraminifera. We chose our standard respiration rate of  $0.41 \text{ nmol CO}_2 \text{ h}^{-1}$  based on laboratory measurements by Nomaki et al. (2007) on *C. wuellerstorfi*, which is one of the preferred species for reconstructing  $\delta^{13}\text{C}$  of past water masses. This respiration rate lies towards the upper end of rates measured for benthic foraminiferal species (in  $\text{nmol CO}_2 \text{ h}^{-1}$ ): 0.33 to 0.63 (Hannah et al., 1994), 0.04 to 0.41 (Nomaki et al., 2007), and  $<0.01$  to 0.23 (Geslin et al., 2011), but is one of the few measurements on deep-sea species. Our standard calcification rate of  $0.28 \text{ nmol C h}^{-1}$  is based on in-culture measurements by Glas et al. (2012) on *Ammonia* sp. Brünnich 1772, a shallow-water symbiont-barren benthic species. To our knowledge this represents the only calcification rate measurement on benthic foraminifera.

**Table 1**

Pressure dependent coefficients for the dissociation constants of acids in seawater, after Millero (1995). For boric acid,  $a_2 \times 10^3$  has been changed from 2.608 to  $-2.608$  ( $\text{m}^3 \text{ }^\circ\text{C}^{-2} \text{ mol}^{-1}$ ) (Rae et al., 2011).

Acid	$-a_0$ $\text{m}^3 \text{ mol}^{-1}$	$a_1$ $\text{m}^3 \text{ }^\circ\text{C}^{-1} \text{ mol}^{-1}$	$a_2 \times 10^3$ $\text{m}^3 \text{ }^\circ\text{C}^{-2} \text{ mol}^{-1}$	$-b_0$ $\text{m}^3 \text{ Pa}^{-1} \text{ mol}^{-1}$	$b_1$ $\text{m}^3 \text{ Pa}^{-1} \text{ }^\circ\text{C}^{-1} \text{ mol}^{-1}$
$\text{H}_2\text{CO}_3$	25.50	0.1271		3.08	0.0877
$\text{HCO}_3^-$	15.82	$-0.0219$		$-1.13$	$-0.1475$
$\text{B}(\text{OH})_3$	29.48	$-0.1622$	$-2.608$	2.84	
$\text{H}_2\text{O}$	25.60	0.2324	$-3.6246$	5.13	0.0794
$\text{HSO}_4^-$	18.03	0.0466	0.316	4.53	0.0900

**Table 2**  
Standard model parameters used in this study.

Parameter	Units	Value
Temperature	°C	1.3
Salinity		34.7
Pressure	bar	300
pH		7.9
$\delta^{13}\text{C}_{\text{DIC}}$	‰	0.5
$\delta^{13}\text{C}_{\text{POC}}$	‰	−21.9
Total alkalinity (TA)	$\mu\text{mol kg}^{-1}$	2400
Radius	$\mu\text{m}$	200
Surface area	$\mu\text{m}^2$	$5.03 \times 10^5$
Volume	$\mu\text{m}^3$	$3.35 \times 10^7$
Biovolume <sup>a</sup>	$\mu\text{m}^3$	$2.51 \times 10^7$
Biomass <sup>b</sup>	$\mu\text{g C}$	2.51
Respiration rate (RR)	$\text{nmol CO}_2 \text{ h}^{-1}$	0.41
RR per biovolume	$\text{nmol CO}_2 \text{ h}^{-1} \mu\text{m}^{-3}$	$1.63 \times 10^{-8}$
RR per biomass	$\text{nmol CO}_2 \text{ h}^{-1} (\mu\text{g C})^{-1}$	0.16
Calcification rate (CR) <sup>c</sup>	$\text{nmol CO}_3^{2-} \text{ h}^{-1}$	0.28
CR per surface area	$\text{nmol CO}_3^{2-} \text{ h}^{-1} \mu\text{m}^{-2}$	$5.57 \times 10^{-7}$

<sup>a</sup> Volume-to-biovolume conversion factor of 0.75 based on Hannah et al. (1994) and Geslin et al. (2011).

<sup>b</sup> Biovolume-to-biomass conversion factor of  $10^{-7}$  ( $\mu\text{g C}$ )  $\mu\text{m}^{-3}$ , based on average of Turley et al. (1986) and Michaels et al. (1995).

<sup>c</sup> Also applies to uptake of  $\text{HCO}_3^-$ .

**Table 3**  
Model parameters used in the different scenarios.

Parameter	Units	Standard	Glacial	Phytodet.
Temperature	°C	1.3	−1.2	1.3
pH		7.9	8.0	7.8
Resp. rate	$\text{nmol CO}_2 \text{ h}^{-1}$	0.41	0.41	0.82

### 2.3. Combined scenarios: the glacial, phytodetritus layer

The scenarios considered in this study are a control scenario for a generic deep ocean setting, a glacial scenario and a phytodetritus layer environment scenario. The changes in the different model parameters associated with the scenarios are shown in Table 3. Changes in  $\delta^{13}\text{C}_{\text{DIC}}$  are not considered, since the model faithfully records those changes in the shell's final  $\delta^{13}\text{C}_{\text{foram}}$  (see Section 3.1). Here we focus on the remaining parameters, which are less well studied. For our glacial scenario we changed two parameters: temperature from 1.3 °C to −1.2 °C (following the temperature reconstructions of Adkins et al., 2002) and pH from 7.9 to 8.0 (Hönisch et al., 2008).

Unfortunately, not much is known about phytodetritus layers on the sea floor. The most extensive review by Beaulieu (2002) has only limited information on chemical composition of these layers. Beaulieu (2002) cites a few measurements of  $\delta^{13}\text{C}_{\text{POC}}$  ranging from −24‰ in the Atlantic sector of the Southern Ocean to −31‰ in the Mediterranean Sea. Furthermore, she reviews the availability of measurements on organic material, C:N ratios and inorganic content, but none is available in as much detail as would be needed for our model input. Therefore our phytodetritus scenario is based on best guesses for pH: during remineralisation and biodegradation, more  $\text{CO}_2$  is released in and around the phytodetritus layer, lowering pH (here we reduce pH by 0.1 to 7.8). For the chosen respiration rate there is, again, not much quantitative information available, rather it has been observed that benthic foraminifera feed on phytodetrital layers and then start new chamber formation or reproduction (Gooday et al., 1990), all of which increase respiration. We therefore doubled the respiration rate to  $0.82 \text{ nmol CO}_2 \text{ h}^{-1}$ .

## 3. Results

Our results are presented in three subsections – one for environmental parameters, one for vital parameters and one for the combined scenarios. If not stated otherwise, the standard model parameters shown in Table 2 apply. Figures in this section show both  $\text{CO}_3^{2-}$  uptake and  $\text{HCO}_3^-$  uptake. The final  $\delta^{13}\text{C}_{\text{foram}}$  for  $\text{CO}_3^{2-}$  uptake is generally higher by 0.07 to 0.08‰ compared to  $\text{HCO}_3^-$  uptake, except for the vital effect sensitivities (see Section 4.3 below). If not mentioned otherwise, the description of the results refers to  $\text{CO}_3^{2-}$  uptake. Table 4 gives an overview of the different sensitivities found in this study.

### 3.1. Environmental parameters

Changes in  $\delta^{13}\text{C}_{\text{DIC}}$  result in changes of exactly the same magnitude in  $\delta^{13}\text{C}_{\text{foram}}$ . There is, however, an offset of around 0.24‰ below the 1:1 line at standard model parameters (see Fig. 2). Increases in temperature by 1 °C cause an increase in  $\delta^{13}\text{C}_{\text{foram}}$  of 0.05‰. The effect of salinity on  $\delta^{13}\text{C}_{\text{foram}}$  is 0.01‰ for  $\Delta S = 5$ . Increasing pressure leads to a drop of  $\delta^{13}\text{C}_{\text{foram}}$  by 0.02 to 0.03‰ per 100 bar (equivalent to 1 km water depth). Increasing  $\delta^{13}\text{C}_{\text{POC}}$  by 10‰ leads to an enrichment of  $\delta^{13}\text{C}_{\text{foram}}$  by only 0.06‰ (Fig. 3). Generally there is a drop in  $\delta^{13}\text{C}_{\text{foram}}$  when pH increases. At low pH values this drop is strongest at −0.08‰ per 0.1 pH increase before dropping to an average of −0.02‰ per

**Table 4**  
Overview of  $\delta^{13}\text{C}_{\text{foram}}$  sensitivity to different model parameters.

Effect of ...	given change of ...	on $\delta^{13}\text{C}_{\text{foram}}$	Fig.
$\delta^{13}\text{C}_{\text{DIC}}$	+ 1‰	+ 1.0‰	2
Temperature	+ 1 °C	+ 0.05‰	2
Salinity	+ 5	<− 0.01‰	2
Pressure	+ 100 bar	− 0.03‰ at lower pressure − 0.02‰ at higher pressure	2
$\delta^{13}\text{C}_{\text{POC}}$	+ 10‰	+ 0.06‰	3
pH	+ 0.1	− 0.08‰ at lower pH − 0.02‰ at higher pH	3
TA	+ 100 $\mu\text{mol kg}^{-1}$	+ 0.01‰	3
Resp. rate	+ 1 $\text{nmol CO}_2 \text{ h}^{-1}$	− 0.36‰ at lower rates − 0.28‰ at higher rates	4
Calc. rate	+ 1 $\text{nmol CO}_3^{2-} \text{ h}^{-1}$	+ 0.08‰ at lower rates + 0.27‰ at higher rates	4
Calc. rate	+ 1 $\text{nmol HCO}_3^- \text{ h}^{-1}$	+ 0.01‰	4

0.1 pH increase at pH values greater than 8.2. Changes in TA have a small impact of + 0.01‰ on  $\delta^{13}\text{C}_{\text{foram}}$  for an increase of 100  $\mu\text{mol kg}^{-1}$ .

### 3.2. Vital parameters

Increasing respiration rates result in more depleted  $\delta^{13}\text{C}_{\text{foram}}$ . The effect is strongest at low respiration rates where an increase of 1  $\text{nmol CO}_2 \text{ h}^{-1}$  causes a decrease of 0.36‰ compared to only 0.28‰ at higher rates (Fig. 4). The fact that respiration rates higher than 2.5  $\text{nmol CO}_2 \text{ h}^{-1}$  are not possible for uptake of  $\text{CO}_3^{2-}$  will be discussed in Section 4.3 below. For increasing calcification rates  $\delta^{13}\text{C}_{\text{foram}}$  gets more enriched. In the case of  $\text{CO}_3^{2-}$  uptake the enrichment is + 0.08‰ per  $\text{nmol CO}_3^{2-} \text{ h}^{-1}$  at low calcification rates and + 0.27‰ per  $\text{nmol CO}_3^{2-} \text{ h}^{-1}$  at rates of 0.5 to 0.6  $\text{nmol CO}_3^{2-} \text{ h}^{-1}$ . For  $\text{HCO}_3^-$  uptake, the enrichment is linear at 0.01‰ per  $\text{nmol HCO}_3^- \text{ h}^{-1}$ . Again,  $\text{CO}_3^{2-}$  uptake is limited: calcification rates higher than 0.6  $\text{nmol CO}_3^{2-} \text{ h}^{-1}$  are not possible in the model.

### 3.3. Combined scenarios

The combined effects of the two scenarios (glacial and phytodetritus layer) on the  $\delta^{13}\text{C}_{\text{foram}}$  values are summarised in Table 5. The combined effects of the individual parameters are − 0.15‰ and − 0.09‰ for the glacial and the phytodetritus scenario, respectively.

## 4. Discussion

### 4.1. General remarks

Many of the laboratory studies that we are using to compare our model results with have been conducted on planktonic foraminifera, which are easier to keep in culture and therefore more attractive experimentation objects. Of course, there are differences between planktonic and benthic foraminiferal species. Erez (2003) predicts that respiration and calcification rates of deep-sea benthics are one to two orders of magnitude lower than those of planktonics. Benthics have much longer life cycles, being able to survive for several years (Hemleben and Kitazato, 1995). In contrast, the lifetime of planktonics is typically of the order of weeks to months, with many life cycles tuned to the lunar cycle (e.g. Bijma et al. (1990, 1994)). The feeding habits and reproduction cycles of deep-sea benthics are different to those of planktonics. Wherever possible, we are using experimental studies on benthics for comparison. Where this is not possible we are taking planktonics bearing in mind the issues mentioned.

One drawback of the model is that it does not include any cell-internal biological features (e.g. internal vacuoles). Neither does it include processes such as vesicular transport within the cell. Accordingly, changes in internal parameters such as the increase in pH of internal vesicles as they are transported to the site of active calcification (e.g. de Nooijer et al. (2009)) cannot be accounted for. These deficiencies as well as the fact that the model has not been validated by a complete set of field data on benthic foraminifera limit the model's predictive

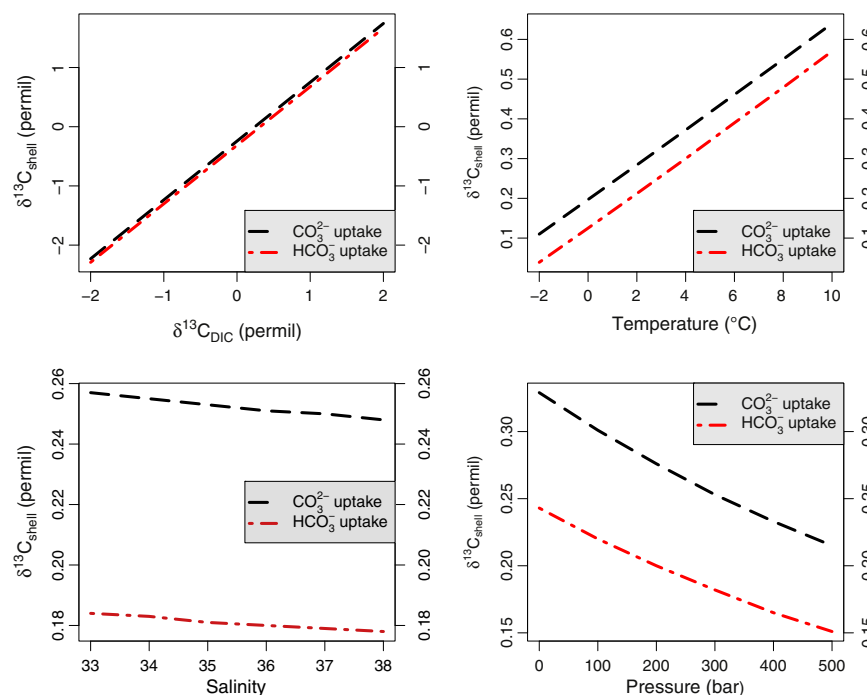


**Fig. 2.** Foraminiferal  $\delta^{13}\text{C}$  for different external model parameters:  $\delta^{13}\text{C}_{\text{DIC}}$ , temperature, salinity and pressure.

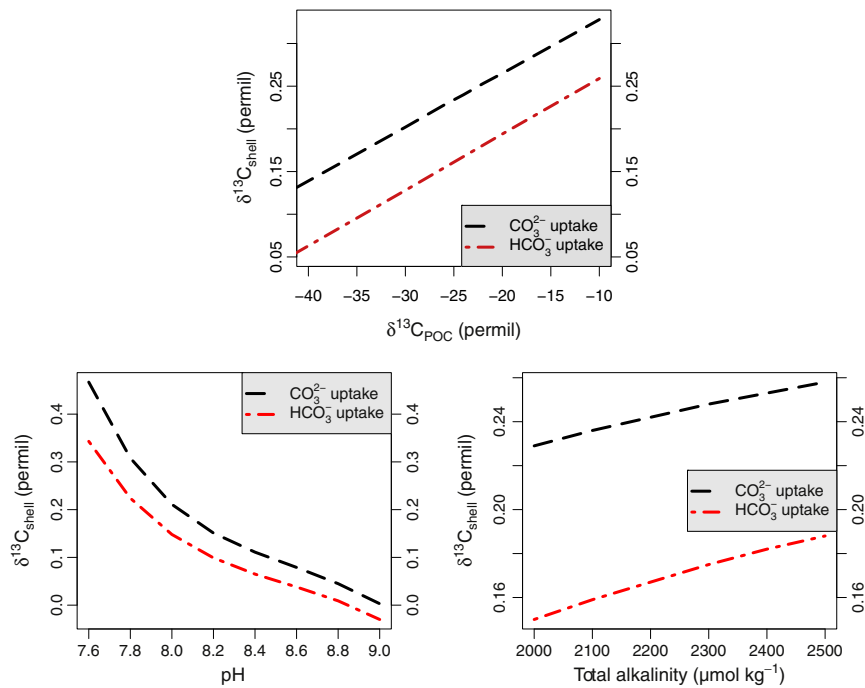


Fig. 3. Same as in Fig. 2 but for  $\delta^{13}\text{C}_{\text{POC}}$ , pH and TA.

power, but we leave the inclusion of internal cell processes and a proper model validation to future studies. Nonetheless, our approach yields some very useful insights into shell-external parameters and the more straightforward vital effects.

#### 4.2. Environmental parameters

In the following subsections we are discussing the various sensitivities in more detail. Salinity and TA are left out, since neither shows a marked effect on  $\delta^{13}\text{C}_{\text{foram}}$ .

##### 4.2.1. $\delta^{13}\text{C}_{\text{DIC}}$

As expected,  $\delta^{13}\text{C}_{\text{DIC}}$  affects  $\delta^{13}\text{C}_{\text{foram}}$  in a 1:1 relationship (Fig. 2). For our standard parameters, however, there is an offset for  $\delta^{13}\text{C}_{\text{foram}}$  of around  $-0.2$  to  $-0.3\%$  with respect to  $\delta^{13}\text{C}_{\text{DIC}}$ . Benthic foraminifera record  $\delta^{13}\text{C}_{\text{DIC}}$  of bottom water or porewater with negative offsets (e.g. Grossman (1987); McCorkle et al. (1990); Rathburn et al. (1996)), but a few epibenthic species such as *C. wuellerstorfi*, in the absence of other effects, capture  $\delta^{13}\text{C}_{\text{DIC}}$  more or less exactly in their  $\delta^{13}\text{C}_{\text{foram}}$  (e.g. Woodruff et al. (1980); Duplessy et al. (1984)). The diffusive

boundary layer above the sediment–water interface adds another complication, as it can be influenced by porewater  $\delta^{13}\text{C}_{\text{DIC}}$  and does not represent bottom water  $\delta^{13}\text{C}_{\text{DIC}}$  only (Zeebe, 2007). Species living inside this diffusive boundary layer may therefore experience a bottom water signal that is influenced by porewater. Species like *C. wuellerstorfi* that tend to live on, or attach themselves to, elevated structures on the seafloor (e.g. Linke and Lutze (1993)) likely escape such porewater influences. For the purpose of this paper  $\delta^{13}\text{C}_{\text{DIC}}$  is taken up into the foraminiferal shell as expected in a 1:1 relationship, even if there is a constant offset. The focus here is on the other parameters that have had less attention in the past.

##### 4.2.2. Temperature

The temperature sensitivity of  $\delta^{13}\text{C}_{\text{foram}}$  is surprisingly high with  $+0.05\%$  per  $^{\circ}\text{C}$ . In the model this is driven (1) by temperature-dependent shifts in the chemical speciation between the different carbonate species and the resulting mass balance constraints on their isotopic composition (with increasing temperature  $\delta^{13}\text{C}_{\text{CO}_2}$  and  $\delta^{13}\text{C}_{\text{CO}_3^{2-}}$  become more enriched, whereas  $\delta^{13}\text{C}_{\text{HCO}_3^{-}}$  more depleted in  $^{13}\text{C}$ ), and (2) by the temperature-related changes of the fractionation

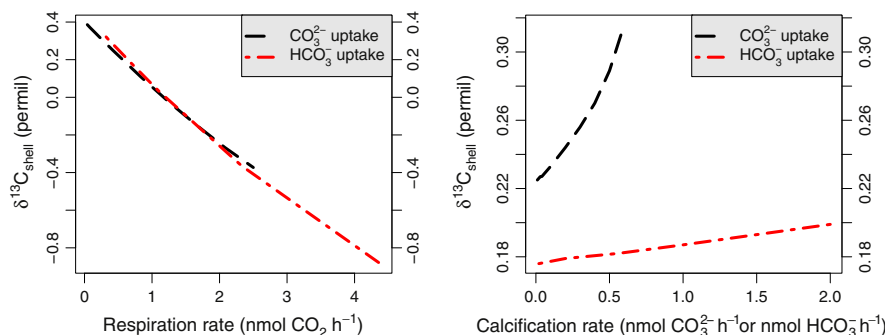


Fig. 4. Foraminiferal  $\delta^{13}\text{C}$  for changes of vital parameters: respiration rate (left) and calcification rate (right).

**Table 5**

Overview of  $\delta^{13}\text{C}_{\text{foram}}$  sensitivity for the two scenarios: glacial and phytodetritus. The combined impact on  $\delta^{13}\text{C}_{\text{foram}}$  may differ from the sum of individual parameter impacts.

Effect of ...	given change of ...	on $\delta^{13}\text{C}_{\text{foram}}$
Glacial combined		−0.15‰
Temperature	−2.5 °C	−0.11‰
pH	+0.1	−0.04‰
Phytodetritus combined		−0.09‰
pH	−0.1	+0.05‰
Respiration rate	+0.41 nmol $\text{CO}_2 \text{ h}^{-1}$	−0.14‰

factors for calcite formation (see Section 2, Mook (1986), and Zeebe et al. (1999)). It is important to mention that there are different measurement values for the fractionation factor between  $\text{CO}_3^{2-}$  and  $\text{CaCO}_3$  (e.g. Lesniak and Sakai (1989); Zhang et al. (1995); Lesniak and Zawadzki (2006)), and that measurements have so far yielded inconclusive results due to varying, and difficult, measurement procedures (Myrntinen et al., 2012). Until consistent measurements emerge, we prefer the traditionally used fractionation factors of Mook (1986).

Laboratory measurements on the symbiont-barren planktonic foraminifer *Globigerina bulloides* show a decrease of  $\delta^{13}\text{C}_{\text{foram}}$  by 0.11‰ per temperature increase of 1 °C (Bemis et al., 2000), which is twice as large and opposite in sign compared to our results. Bemis et al. (2000) hypothesise though that increasing temperatures induce higher respiration rates, which, in turn, introduce more depleted  $\delta^{13}\text{C}_{\text{CO}_2}$  near the shell. After conversion from  $\text{CO}_2$  to  $\text{HCO}_3^-$  and  $\text{CO}_3^{2-}$ , this carbon is subsequently taken up during calcification, thus lowering  $\delta^{13}\text{C}_{\text{foram}}$ . We also find a lowering of  $\delta^{13}\text{C}_{\text{foram}}$  with increasing respiration rates (see Fig. 4), which, depending on the increase in respiration rate, can easily overprint the signal caused by a temperature increase. In fact, our model requires an increase of the standard respiration rate of 0.5 nmol  $\text{CO}_2 \text{ h}^{-1}$  from 0.41 to 0.91 nmol  $\text{CO}_2 \text{ h}^{-1}$  in order to explain Bemis et al. (2000)'s hypothesis. Combined measurements of temperature and respiration would be highly desirable in order to test these results.

#### 4.2.3. Pressure

The pressure effect on  $\delta^{13}\text{C}_{\text{foram}}$  in the model is relatively small with a decrease of only 0.02 to 0.03‰ per increase of 100 bar (equivalent to a

depth increase of 1000 m). The difference in  $\delta^{13}\text{C}_{\text{foram}}$  between a foraminifer living at a depth of 3000 m and 5000 m is therefore only about 0.05 to 0.06‰. Higher pressure causes a shift in the chemical speciation of the carbonate system, such that the concentration of  $\text{CO}_3^{2-}$  is reduced and its  $\delta^{13}\text{C}$  value is lower (qualitatively the opposite effect of increasing temperature). Upon uptake and calcification this lower  $\delta^{13}\text{C}_{\text{CO}_3^{2-}}$  results in an equally depleted  $\delta^{13}\text{C}_{\text{foram}}$ .

#### 4.2.4. $\delta^{13}\text{C}_{\text{POC}}$

$\delta^{13}\text{C}_{\text{POC}}$  varies with latitude (Rau et al., 1989; Goericke and Fry, 1994): at the equator  $\delta^{13}\text{C}_{\text{POC}}$  is typically around −20‰, becoming more negative towards the poles with down to −26‰ in the Northern Hemisphere and −35‰ in the Southern Hemisphere. Differences in the two hemispheres can be explained by differences in temperature,  $[\text{CO}_2(\text{aq})]$  and growth rates (see e.g. Hofmann et al. (2000)). The decrease of  $\delta^{13}\text{C}_{\text{foram}}$  in our model with decreasing values of  $\delta^{13}\text{C}_{\text{POC}}$  (Fig. 3) is expected. Respired  $\text{CO}_2$  in the model is added to the external environment at the foraminifer shell boundary. This is also the area where  $\text{HCO}_3^-$  or  $\text{CO}_3^{2-}$  is taken up by calcification. Conversion between the different carbonate species causes some of the low- $\delta^{13}\text{C}$   $\text{CO}_2$  to become  $\text{HCO}_3^-$  and  $\text{CO}_3^{2-}$ , which is subsequently taken up into the foraminifer shell, thus lowering  $\delta^{13}\text{C}_{\text{foram}}$ . Fig. 5 demonstrates the effect of lower  $\delta^{13}\text{C}_{\text{POC}}$  on the  $\delta^{13}\text{C}$  values of the different carbon species as well as  $\Sigma \text{CO}_2$ . For standard model parameters the change in  $\delta^{13}\text{C}_{\text{foram}}$  per change of  $\delta^{13}\text{C}_{\text{POC}}$  is around 0.6‰, i.e.  $\delta^{13}\text{C}_{\text{foram}}$  changes by only 0.06‰ in response to a 10‰ change in  $\delta^{13}\text{C}_{\text{POC}}$ . In laboratory experiments Spero and Lea (1996) fed planktonic *G. bulloides* algal diets of differing  $\delta^{13}\text{C}_{\text{POC}}$  values. This caused a marked effect in the  $\delta^{13}\text{C}_{\text{foram}}$  values. Their observed change in  $\delta^{13}\text{C}_{\text{foram}}$  per change of  $\delta^{13}\text{C}_{\text{POC}}$  is around 3.5‰, which is more than five times higher than our model results suggest. In the model the carbon has to take a detour via release of low  $\delta^{13}\text{C}_{\text{CO}_2}$ , subsequent conversion to  $\text{HCO}_3^-$  and  $\text{CO}_3^{2-}$ , and finally uptake and inclusion into the shell during calcification. If the metabolic  $\text{CO}_2$  derived from depleted  $\delta^{13}\text{C}_{\text{POC}}$  is transferred into the shell via an internal pathway (for instance via an internal “carbon pool”, e.g. Bijma et al. (1999)), this may be more efficient in transmitting the  $\delta^{13}\text{C}_{\text{POC}}$  signal into the shell's  $\delta^{13}\text{C}_{\text{foram}}$ .

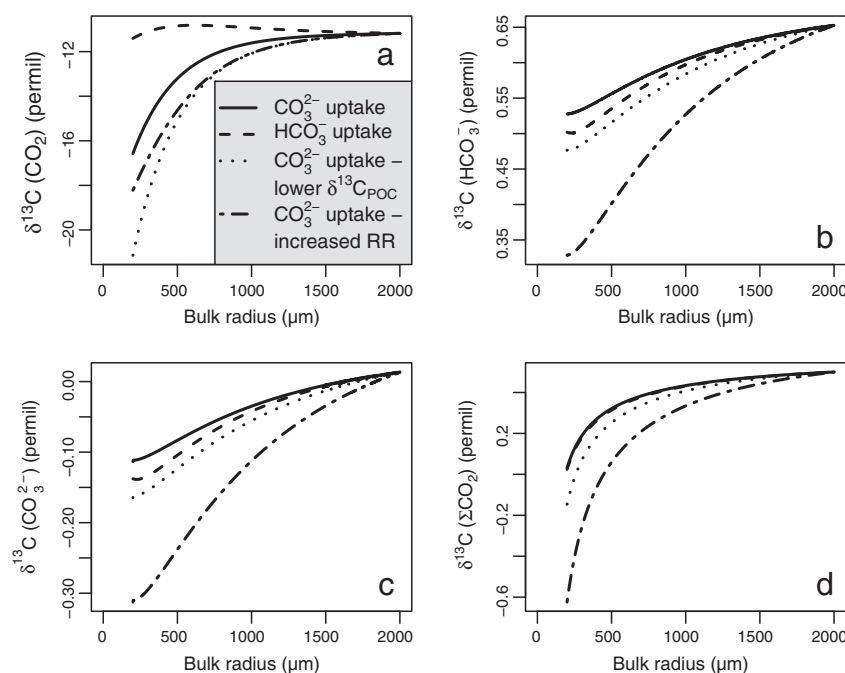


**Fig. 5.** Model results for the  $\delta^{13}\text{C}$  of  $\text{CO}_2$  (a),  $\text{HCO}_3^-$  (b),  $\text{CO}_3^{2-}$  (c), and  $\Sigma \text{CO}_2$  (d). The solid line represents  $\text{CO}_3^{2-}$  uptake at 0.28 nmol  $\text{CO}_3^{2-} \text{ h}^{-1}$ , the dashed line is  $\text{HCO}_3^-$  uptake at 0.56 nmol  $\text{HCO}_3^- \text{ h}^{-1}$  (same net calcification rate as for  $\text{CO}_3^{2-}$  uptake), the dotted line is  $\text{CO}_3^{2-}$  uptake with  $\delta^{13}\text{C}_{\text{POC}}$  reduced from −21.9 to −30.0‰, and the dash-dotted line is  $\text{CO}_3^{2-}$  uptake at an increased respiration rate of 1.0 nmol  $\text{CO}_3^{2-} \text{ h}^{-1}$ .

#### 4.2.5. pH

The effect of pH on  $\delta^{13}\text{C}_{\text{foram}}$  is more pronounced at pH values below 8, but is generally less than  $+0.1\%$  per 0.1 pH decrease (see Fig. 3). In the model this is achieved by a shift in the chemical speciation and the associated mass balance constraints on the isotopic composition (cf. discussion on temperature and pressure above). Measurements on endobenthic *Oridorsalis umbonatus* by Rathmann and Kuhner (2008) yield inconclusive results for a possible pH effect on  $\delta^{13}\text{C}_{\text{foram}}$ . The effect in the model is smaller than what was found by Spero et al. (1997) in planktonic foraminifera: they measured a change in  $\delta^{13}\text{C}_{\text{foram}}$  by  $-0.32\%$  per 0.1 pH unit increase for *Orbulina universa* and  $-0.75\%$  for *G. bulloides*. This suggests that the model may not fully capture the pH/carbonate ion effect and its likely associated biological mechanism. The pH at the actual calcification site may be different, notably higher (e.g. de Nooijer et al. (2009)). The neglect of cell-internal processes in the model – we only consider the pH-driven fractionation between the carbonate species at the outer boundary of the shell – is most probably responsible for the weak simulated pH effect.

### 4.3. Vital parameters

#### 4.3.1. Respiration rate

The respiration rate is the second most sensitive model parameter affecting  $\delta^{13}\text{C}_{\text{foram}}$  after  $\delta^{13}\text{C}_{\text{DIC}}$  (see Fig. 4). An averaged decrease of  $0.3\%$  per increase of  $1 \text{ nmol CO}_2 \text{ h}^{-1}$  adds a further challenge for interpreting  $\delta^{13}\text{C}_{\text{foram}}$ . In the model this is caused by more low- $\delta^{13}\text{C}$   $\text{CO}_2$  which is diffusing out of the foraminifer. In turn, this is lowering the  $\delta^{13}\text{C}$  values of  $\text{HCO}_3^-$  and  $\text{CO}_3^{2-}$ , either of which are taken up during calcification, and resulting in depleted  $\delta^{13}\text{C}_{\text{foram}}$  values. Fig. 5 illustrates the changes in  $\delta^{13}\text{C}$  of the different carbon species for increased respiration rates. For calcification with  $\text{CO}_3^{2-}$ , respiration rates higher than  $2.5 \text{ nmol CO}_2 \text{ h}^{-1}$  are not possible, since the increased concentration of  $\text{CO}_2$  causes an overall drop of pH near the shell, thus lowering and eventually depleting all remaining  $\text{CO}_3^{2-}$ . How important is this effect? In this context it would be beneficial to know under which conditions foraminifera increase their metabolism and respire more. Several studies on benthic foraminifera have shown that they are dormant for most

of the year, but increase their activity as soon as food is available (e.g. Moodley et al. (2002)). At this time they also build their new chambers and/or reproduce. To our knowledge, in-situ measurements of respiration rates on deep-sea benthic foraminifera do not exist. Measurements on cultured benthic species vary across two orders of magnitude (Geslin et al., 2011). Given the strong impact that respiration rates have on  $\delta^{13}\text{C}_{\text{foram}}$  in our model, measurements of respiration rates before, during, and after chamber formation would be highly desirable to improve our understanding of  $\delta^{13}\text{C}_{\text{foram}}$  signal formation.

#### 4.3.2. Calcification rate and $\text{CO}_3^{2-}$ vs. $\text{HCO}_3^-$ uptake

The sensitivity of  $\delta^{13}\text{C}_{\text{foram}}$  in response to changing calcification rates is less than  $0.1\%$ , which is significantly lower than for changing respiration rates. At standard model parameters  $\text{CO}_3^{2-}$  uptake rates can only be as high as  $0.6 \text{ nmol h}^{-1}$  since at higher rates the  $\text{CO}_3^{2-}$  pool near the modelled shell boundary is depleted (see Fig. 6). When bulk pH is increased,  $[\text{CO}_3^{2-}]$  also increases allowing for higher calcification rates. In contrast, uptake of  $\text{HCO}_3^-$  is not restricted since  $\text{HCO}_3^-$  is not limiting. The associated changes in  $\delta^{13}\text{C}_{\text{foram}}$  for  $\text{HCO}_3^-$  uptake are small compared to many of the other parameters tested in this study. Our model results generally suggest that  $\text{HCO}_3^-$  uptake results in  $\delta^{13}\text{C}_{\text{foram}}$  values that are lower by 0.07 to 0.08‰ compared to  $\text{CO}_3^{2-}$  uptake. This seems counter-intuitive as  $\delta^{13}\text{C}_{\text{HCO}_3^-}$  is more than 0.6‰ higher than  $\delta^{13}\text{C}_{\text{CO}_3^{2-}}$  (Fig. 5). The simple explanation is that at  $1.3 \text{ }^\circ\text{C}$  the fractionation factor between  $\text{HCO}_3^-$  and  $\text{CaCO}_3$  is  $-0.32\%$ , whereas for  $\text{CO}_3^{2-}$  and  $\text{CaCO}_3$  it is  $+0.37\%$ , thus offsetting the differences in  $\delta^{13}\text{C}$  of the two carbon species near the shell. Which of the two carbon species is actually taken up during calcification of foraminifera has still not been established. The obvious choice seems to be  $\text{CO}_3^{2-}$  following the simple calcification equation



Modelling results for the planktonic species *Globigerinoides sacculifer*, however, have shown that carbonate ion supply can be insufficient to account for measured calcification rates (Wolf-Gladrow et al., 1999), just as for our results at rates higher than  $0.6 \text{ nmol CO}_3^{2-} \text{ h}^{-1}$ .

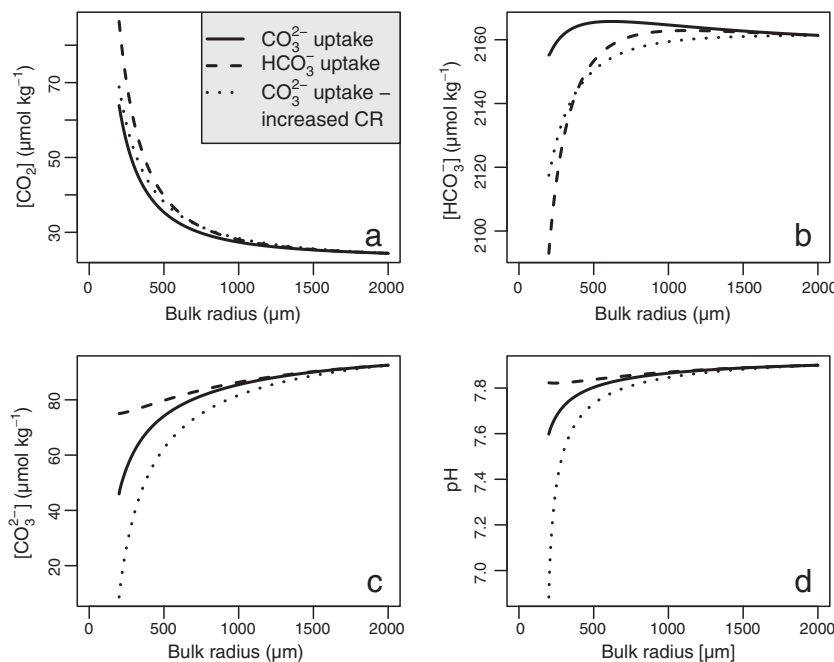


**Fig. 6.** Model results for the bulk concentrations of  $\text{CO}_2$  (a),  $\text{HCO}_3^-$  (b),  $\text{CO}_3^{2-}$  (c), and pH (d). The solid line represents  $\text{CO}_3^{2-}$  uptake at  $0.28 \text{ nmol CO}_3^{2-} \text{ h}^{-1}$ , the dashed line is  $\text{HCO}_3^-$  uptake at  $0.56 \text{ nmol HCO}_3^- \text{ h}^{-1}$  (same net calcification rate as for  $\text{CO}_3^{2-}$  uptake), and the dotted line is  $\text{CO}_3^{2-}$  uptake at an increased rate of  $0.60 \text{ nmol CO}_3^{2-} \text{ h}^{-1}$ . At this elevated calcification rate the  $\text{CO}_3^{2-}$  concentration at the shell boundary is approaching zero (c) – higher rates are physically not possible.

Therefore some foraminifera may require an internal carbon pool (e.g. Erez (2003)) from which carbon is taken during calcification, or partly (maybe fully) employ bicarbonate ion:



Another process to overcome the depletion of the carbonate ion pool near the shell is the elevation of internal pH (e.g. de Nooijer et al. (2009)). This could create a sufficiently high concentration of carbonate ions inside the foraminifer which is supplied by uptake and subsequent conversion of  $\text{HCO}_3^-$  and/or  $\text{CO}_2$  to  $\text{CO}_3^{2-}$ . Yet another mechanism could be the foraminifer's pseudopodial network that can reach out into the ambient seawater and harvest more  $\text{CO}_3^{2-}$  from a bigger volume than would be possible by simple cross-membrane transport at the shell boundary. Here we cannot answer which of these mechanisms is at work. The model results suggest though that one or more of the described mechanisms is needed in order to allow the foraminifer to calcify at rates greater than  $0.6 \text{ nmol h}^{-1}$  when using  $\text{CO}_3^{2-}$ .

#### 4.4. Combined scenarios

##### 4.4.1. The glacial

Our glacial results (Table 5) suggest that we may explain 33 to 47% of the observed interglacial to glacial drop in  $\delta^{13}\text{C}_{\text{foram}}$  (based on the global ocean average of  $-0.46\%$  (Curry et al., 1988) to  $-0.32\%$  (Duplessy et al., 1988)) by changes in temperature and pH. Temperature is the main driver in our model, whereas the carbonate ion effect (or pH effect) has a relatively minor impact. The carbonate ion effect in some planktonic foraminifera found by Spero et al. (1997) also serves as a possible explanation for lowered  $\delta^{13}\text{C}_{\text{foram}}$  during the glacial (see also Lea et al. (1999)). To our knowledge the temperature– $\delta^{13}\text{C}_{\text{foram}}$  relationship has not been assessed before for benthic foraminifera in the context of glacial–interglacial changes.

The reduced drop in  $\delta^{13}\text{C}_{\text{DIC}}$  on glacial–interglacial timescales, as implied by our model results, would reduce the amount of terrestrial carbon that was predicted to be transferred into the glacial ocean (Shackleton, 1977) by several hundred gigatonnes. Such a reduced carbon transfer would result in a less intense carbonate dissolution event and limit the subsequent shoaling of the  $\text{CaCO}_3$  saturation horizon, thus potentially allowing for more  $\text{CO}_2$  to be taken up by the glacial ocean (Broecker, 2005). Our findings further exacerbate the already big discrepancy between foraminiferal  $\delta^{13}\text{C}$  and pollen data on the amount of terrestrial carbon transferred into the ocean (Crowley, 1995). Here, we only want to hint at some of the possible consequences rather than trying to fully explain the glacial ocean and glacial  $\text{CO}_2$ , which is beyond the scope of this paper.

Admittedly, our 'one-size-fits-all' approach to the glacial is a bit rough: Different core sites have of course experienced different parameter changes during the glacial and each core needs to be looked at in detail. Deep ocean temperatures have not decreased everywhere by our assumed  $2.5 \text{ }^\circ\text{C}$  (based on Adkins et al. (2002)). The same is true for pH: Hönisch et al. (2008) found that pH in the southeast Atlantic Ocean during the LGM was increased by up to 0.1 pH units above 3500 m water depth, but decreased below that depth ( $-0.07$  pH units). The Pacific may have experienced increases of up to 0.5 pH units (Sanyal et al., 1997). A logical next step would be to apply our model to a combined carbon cycle/general ocean circulation model in order to obtain spatial patterns for  $\delta^{13}\text{C}_{\text{foram}}$ . These could then be compared to observational data from sediment cores (e.g. Oliver et al. (2010)), comparable to the approach of Hesse et al. (2011), and allow for a more nuanced interpretation of possible glacial implications of our findings.

##### 4.4.2. Phytodetritus layer

So far most of the effect of a phytodetritus layer was attributed to lowering of  $\delta^{13}\text{C}_{\text{DIC}}$  in the layer's interstitial waters due to

remineralisation of low- $\delta^{13}\text{C}$  organic material (e.g. Mackensen et al. (1993)). Our result of  $-0.09\%$  (Table 5) allows us to explain about a quarter of the typical reduction of  $-0.4\%$  found in some phytodetritus layer locations (see e.g. Bickert and Mackensen (2004); Zarriss and Mackensen (2011)) without invoking changes in  $\delta^{13}\text{C}_{\text{DIC}}$ . The increased respiration rate is the main driver in our model. Whether or not a doubling of the respiration rate to  $0.82 \text{ nmol CO}_2 \text{ h}^{-1}$  is realistic cannot be said for certain, since the available respiration rate measurements have all been taken in experimental conditions without added food (Hannah et al., 1994; Nomaki et al., 2007; Geslin et al., 2011). Further respiration rate measurements before, during, and after feeding foraminifera are therefore highly desirable.

## 5. Conclusions

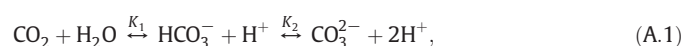
The objective of this study is to test the sensitivity of  $\delta^{13}\text{C}$  in benthic foraminiferal shells to different physical, chemical and biological parameters using a reaction diffusion model for calcification of foraminifera. Changes in  $\delta^{13}\text{C}_{\text{DIC}}$  cause equal changes in  $\delta^{13}\text{C}_{\text{foram}}$  in the model. Offsets between  $\delta^{13}\text{C}_{\text{DIC}}$  and  $\delta^{13}\text{C}_{\text{foram}}$  depend on a variety of physical, chemical and biological parameters. Our results show that temperature, respiration rate and pH potentially have a marked effect on  $\delta^{13}\text{C}_{\text{foram}}$ , whereas salinity, pressure,  $\delta^{13}\text{C}_{\text{POC}}$ , total alkalinity and calcification rate are less important. The model can potentially account for 33 to 47% of the drop in glacial  $\delta^{13}\text{C}_{\text{foram}}$  with respect to Holocene values by a combination of lower temperature and higher pH, with temperature causing most of the signal. This finding may require a re-interpretation of  $\delta^{13}\text{C}_{\text{foram}}$  on glacial–interglacial timescales, as it implies that glacial deep ocean  $\delta^{13}\text{C}_{\text{DIC}}$  was higher than previously thought. We may explain about a quarter of the decrease in  $\delta^{13}\text{C}_{\text{foram}}$  of foraminifera living in and feeding on phytodetrital layers without invoking changes in  $\delta^{13}\text{C}_{\text{DIC}}$ . Critically, this decrease is depending on the respiration rate, for which we have no measurement data. Possible future uses of the model include the application to coupled carbon cycle/general ocean circulation models in order to assess spatial patterns, or a closer look at ontogenetic processes and the associated  $\delta^{13}\text{C}_{\text{foram}}$  changes.

## Acknowledgements

TH would like to thank Martin Glas, Nina Keul and Lennart de Nooijer for helpful discussions. Earlier versions of this manuscript have been substantially improved by suggestions from Frans Jorissen (editor) and three reviewers. Financial support from the Helmholtz Graduate School for Polar and Marine Research (POLMAR) is gratefully acknowledged.

## Appendix A

In equilibrium the individual carbonate species are related by:



where  $K_1$  and  $K_2$  are the equilibrium or dissociation constants. They are given by

$$K_1 = \frac{[\text{HCO}_3^-][\text{H}^+]}{[\text{CO}_2]} \quad (\text{A.2})$$

and

$$K_2 = \frac{[\text{CO}_3^{2-}][\text{H}^+]}{[\text{HCO}_3^-]}, \quad (\text{A.3})$$

and depend on temperature, pressure and salinity. The chemical

reactions for the carbonate system are:



where  $k_+$  and  $k_-$  are the reaction rate constants for the forward and backward reactions, respectively. The general form of the equations for the concentration  $c(r, t)$  of a carbonate system species in the foraminifer model is (as before):

$$0 = \frac{\partial c(r, t)}{\partial t} = \text{Diffusion} + \text{Reaction} + \text{Uptake},$$

where  $r$  is the distance from the centre of the shell and  $t$  is time. The full diffusion–reaction equations for total carbon ( $C = {}^{13}\text{C} + {}^{12}\text{C}$ ) are (Wolf-Gladrow et al., 1999):

For  $\text{CO}_2$ :

$$0 = \frac{D_{\text{CO}_2}}{r^2} \frac{d}{dr} \left( r^2 \frac{d[\text{CO}_2]}{dr} \right) + (k_{-1}[\text{H}^+] + k_{-4})[\text{HCO}_3^-] - (k_{+1} + k_{+4}[\text{OH}^-])[\text{CO}_2], \quad (\text{A.9})$$

where  $D_{\text{CO}_2}$  is the diffusion coefficient of  $\text{CO}_2$  in seawater and the reaction rate constants are  $k_i$ . Likewise for  $\text{HCO}_3^-$ :

$$0 = \frac{D_{\text{HCO}_3^-}}{r^2} \frac{d}{dr} \left( r^2 \frac{d[\text{HCO}_3^-]}{dr} \right) + k_{+1}[\text{CO}_2] - k_{-1}[\text{H}^+][\text{HCO}_3^-] + k_{+4}[\text{CO}_2][\text{OH}^-] - k_{-4}[\text{HCO}_3^-] + k_{+5}[\text{H}^+][\text{CO}_3^{2-}] - k_{-5}[\text{HCO}_3^-], \quad (\text{A.10})$$

for  $\text{CO}_3^{2-}$ :

$$0 = \frac{D_{\text{CO}_3^{2-}}}{r^2} \frac{d}{dr} \left( r^2 \frac{d[\text{CO}_3^{2-}]}{dr} \right) + k_{-5}[\text{HCO}_3^-] - k_{+5}[\text{H}^+][\text{CO}_3^{2-}], \quad (\text{A.11})$$

for  $\text{H}^+$ :

$$0 = \frac{D_{\text{H}^+}}{r^2} \frac{d}{dr} \left( r^2 \frac{d[\text{H}^+]}{dr} \right) + (k_{-5} - k_{-1}[\text{H}^+][\text{HCO}_3^-] + k_{+1}[\text{CO}_2] - k_{+5}[\text{H}^+][\text{CO}_3^{2-}] + k_{+6} - k_{-6}[\text{H}^+][\text{OH}^-] + k_{+7}[\text{B(OH)}_3] - k_{-7}[\text{H}^+][\text{B(OH)}_4^-]), \quad (\text{A.12})$$

for  $\text{OH}^-$ :

$$0 = \frac{D_{\text{OH}^-}}{r^2} \frac{d}{dr} \left( r^2 \frac{d[\text{OH}^-]}{dr} \right) + k_{-4}[\text{HCO}_3^-] - k_{+4}[\text{CO}_2][\text{OH}^-] + k_{+6} - k_{-6}[\text{H}^+][\text{OH}^-], \quad (\text{A.13})$$

for  $\text{B(OH)}_3$ :

$$0 = \frac{D_{\text{B(OH)}_3}}{r^2} \frac{d}{dr} \left( r^2 \frac{d[\text{B(OH)}_3]}{dr} \right) - k_{+7}[\text{B(OH)}_3] - k_{-7}[\text{H}^+][\text{B(OH)}_4^-], \quad (\text{A.14})$$

and for  $\text{B(OH)}_4^-$ :

$$0 = \frac{D_{\text{B(OH)}_4^-}}{r^2} \frac{d}{dr} \left( r^2 \frac{d[\text{B(OH)}_4^-]}{dr} \right) - k_{+7}[\text{B(OH)}_3] - k_{-7}[\text{H}^+][\text{B(OH)}_4^-]. \quad (\text{A.15})$$

For the  $^{13}\text{C}$  calculations, only the reactions for  $^{13}\text{CO}_2$ ,  $\text{H}^{13}\text{CO}_3^-$  and  $^{13}\text{CO}_3^{2-}$  need to be considered (Zeebe et al., 1999):

For  $^{13}\text{CO}_2$ :

$$0 = \frac{D_{^{13}\text{CO}_2}}{r^2} \frac{d}{dr} \left( r^2 \frac{d[^{13}\text{CO}_2]}{dr} \right) + (k'_{-1} [\text{H}^+] + k'_{-4}) [\text{H}^{13}\text{CO}_3^-] - (k'_{+1} + k'_{+4} [\text{OH}^-]) [^{13}\text{CO}_2], \quad (\text{A.16})$$

for  $\text{H}^{13}\text{CO}_3^-$ :

$$0 = \frac{D_{\text{H}^{13}\text{CO}_3^-}}{r^2} \frac{d}{dr} \left( r^2 \frac{d[\text{H}^{13}\text{CO}_3^-]}{dr} \right) + (k'_{+1} [^{13}\text{CO}_2] + k'_{-1}) [\text{H}^+] [\text{H}^{13}\text{CO}_3^-] + k'_{+4} [^{13}\text{CO}_2] [\text{OH}^-] - k'_{-4} [\text{H}^{13}\text{CO}_3^-] + k'_{+5} [\text{H}^+] [^{13}\text{CO}_3^{2-}] - k'_{-5} [\text{H}^{13}\text{CO}_3^-] \quad (\text{A.17})$$

and for  $^{13}\text{CO}_3^{2-}$ :

$$0 = \frac{D_{^{13}\text{CO}_3^{2-}}}{r^2} \frac{d}{dr} \left( r^2 \frac{d[^{13}\text{CO}_3^{2-}]}{dr} \right) + k'_{-5} [\text{H}^{13}\text{CO}_3^-] - k'_{+5} [\text{H}^+] [^{13}\text{CO}_3^{2-}]. \quad (\text{A.18})$$

The kinetic rate constants for  $^{13}\text{C}$  ( $k'_i$ ) are used to take into account kinetic fractionation effects (see Zeebe et al. (1999) for details).

## Appendix B

For the interested reader, we here provide a simplified equation for predicting  $\delta^{13}\text{C}_{\text{foram}}$ . This presents a quick and easy way to test the influence of the most sensitive model input parameters without the need to actually run the foraminiferal calcification model:

$$\delta^{13}\text{C}_{\text{foram}} = \delta^{13}\text{C}_{\text{DIC}} + a_1 (T - 7 \text{ } ^\circ\text{C}) - a_2 (RR - 0.41 \text{ nmol CO}_2 \text{ h}^{-1}) - a_3 (\text{pH} - 7.9), \quad (\text{B.1})$$

where  $T$  is temperature in  $^\circ\text{C}$ ,  $RR$  is the respiration rate in  $\text{nmol CO}_2 \text{ h}^{-1}$ ,  $a_1$  is 0.045‰ per  $^\circ\text{C}$ ,  $a_2$  is 0.4‰ per  $\text{nmol CO}_2 \text{ h}^{-1}$ , and  $a_3$  is 0.04‰ (for the pH range from 7.8 to 8.2).

## References

- Adkins, J.F., McIntyre, K., Schrag, D.P., 2002. The salinity, temperature, and  $\delta^{18}\text{O}$  of the glacial deep ocean. *Science* 298 (5599), 1769–1773.
- Archer, D., Emerson, S., Smith, C.R., 1989. Direct measurement of the diffusive sublayer at the deep-sea floor using oxygen microelectrodes. *Nature* 340, 623–626.
- Barras, C., Duplessy, J.C., Geslin, E., Michel, E., Jorissen, F.J., 2010. Calibration of  $\delta^{18}\text{O}$  of cultured benthic foraminiferal calcite as a function of temperature. *Biogeosciences* 7, 1349–1356.
- Beaulieu, S.E., 2002. Accumulation and fate of phytodetritus on the sea floor. In: Gibson, R.N., Barnes, M., Atkinson, R.J.A. (Eds.), *Oceanogr. Mar. Biol.* vol. 40. Taylor & Francis, pp. 171–232.
- Bemis, B.E., Spero, H.J., Lea, D.W., Bijma, J., 2000. Temperature influence on the carbon isotopic composition of *Globigerina bulloides* and *Orbulina universa* (planktonic foraminifera). *Mar. Micropaleontol.* 38 (3–4), 213–228.
- Bickert, T., Mackensen, A., 2004. Last Glacial to Holocene changes in South Atlantic deep water circulation. In: Wefer, G., Mulitza, S., Ratmeyer, V. (Eds.), *The South Atlantic in the Late Quaternary: Reconstruction of Material Budgets and Current Systems*. Springer, Berlin, pp. 671–695.
- Bijma, J., Erez, J., Hemleben, C., 1990. Lunar and semi-lunar reproductive cycles in some spinose planktonic foraminifers. *J. Foraminif. Res.* 20 (2), 117–127.
- Bijma, J., Hemleben, C., Wellnitz, K., 1994. Lunar-influenced carbonate flux of the planktonic foraminifer *Globigerinoides sacculifer* (Brady) from the central Red Sea. *Deep-Sea Res.* 41 (3), 511–530.
- Bijma, J., Spero, H.J., Lea, D.W., 1999. Reassessing foraminiferal stable isotope geochemistry: impact of the oceanic carbonate system (experimental results). In: Fischer, G., Wefer, G. (Eds.), *Use of Proxies in Paleoclimatology – Examples from the South Atlantic*. Springer, Berlin, pp. 489–512.
- Broecker, W.S., 2005. *The Role of the Ocean in Climate Yesterday, Today, and Tomorrow*. Edigio Press, New York.
- Chandler, G.T., Williams, D.F., Spero, H.J., Gao, X.D., 1996. Sediment microhabitat effects on carbon stable isotopic signatures of microcosm-cultured benthic foraminifera. *Limnol. Oceanogr.* 41 (4), 680–688.
- Crowley, T.J., 1995. Ice-age terrestrial carbon changes revisited. *Global Biogeochem. Cy.* 9, 377–389.
- Curry, W.B., Oppo, D.W., 2005. Glacial watermass geometry and the distribution of  $\delta^{13}\text{C}$  of  $\Sigma\text{CO}_2$  in the western Atlantic Ocean. *Paleoceanography* 20 (1).
- Curry, W.B., Duplessy, J.C., Labeyrie, L.D., Shackleton, N.J., 1988. Changes in the distribution of  $\delta^{13}\text{C}$  of deep water  $\Sigma\text{CO}_2$  between the last glaciation and the Holocene. *Paleoceanography* 3 (3), 317–341.
- de Nooijer, L.J., Toyofuku, T., Kitazato, H., 2009. Foraminifera promote calcification by elevating their intracellular pH. *Proc. Natl. Acad. Sci. U. S. A.* 106 (36), 15374–15378.
- Duplessy, J.C., Shackleton, N.J., Matthews, R.K., Prell, W., Ruddiman, W.F., Caralp, M., Hendy, C.H., 1984.  $^{13}\text{C}$  record of benthic foraminifera in the last interglacial ocean – implications for the carbon cycle and the global deep-water circulation. *Quat. Res.* 21 (2), 225–243.
- Duplessy, J.C., Shackleton, N.J., Fairbanks, R.G., Labeyrie, L., Oppo, D.W., Kallel, N., 1988. Deepwater source variations during the last climatic cycle and their impact on the global deepwater circulation. *Paleoceanography* 3 (3), 343–360.
- Erez, J., 2003. The source of ions for biomineralization in foraminifera and their implications for paleoceanographic proxies. *Rev. Mineral. Geochem.* 54, 115–149.
- Filipsson, H.L., Bernhard, J.M., Lincoln, S.A., McCorkle, D.C., 2010. A culture-based calibration of benthic foraminiferal paleotemperature proxies:  $\delta^{18}\text{O}$  and Mg/Ca results. *Biogeosciences* 7, 1335–1347.
- Geslin, E., Risgaard-Petersen, N., Lombard, F., Metzger, E., Langlet, D., Jorissen, F., 2011. Oxygen respiration rates of benthic foraminifera as measured with oxygen microsensors. *J. Exp. Mar. Biol. Ecol.* 396 (2), 108–114.
- Glas, M.S., Langer, G., Keul, N., 2012. Calcification acidifies the microenvironment of a benthic foraminifer (*Ammonia* sp.). *J. Exp. Mar. Biol. Ecol.* 424, 53–58.
- Goericke, R., Fry, B., 1994. Variations of marine plankton  $\delta^{13}\text{C}$  with latitude, temperature, and dissolved  $\text{CO}_2$  in the world ocean. *Global Biogeochem. Cy.* 8 (1), 85–90.
- Goody, A.J., Turley, C.M., Allen, J.A., 1990. Responses by benthic organisms to inputs of organic material to the ocean-floor – a review. *Philos. T. Roy. Soc. A* 331 (1616), 119–138.
- Grossman, E.L., 1987. Stable isotopes in modern benthic foraminifera – a study of vital effects. *J. Foraminif. Res.* 17, 48–61.
- Hannah, F., Rogerson, A., Laybournparry, J., 1994. Respiration rates and biovolumes of common benthic foraminifera (Protozoa). *J. Mar. Biol. Assoc. UK* 74 (2), 301–312.
- Havach, S.M., Chandler, G.T., Wilson-Finelli, A., Shaw, T.J., 2001. Experimental determination of trace element partition coefficients in cultured benthic foraminifera. *Geochim. Cosmochim. Acta* 65 (8), 1277–1283.
- Hemleben, C., Kitazato, H., 1995. Deep-sea foraminifera under long-time observation in the laboratory. *Deep-Sea Res.* 42 (6), 827–832.
- Hesse, T., Butzin, M., Bickert, T., Lohmann, G., 2011. A model-data comparison of  $\delta^{13}\text{C}$  in the glacial Atlantic Ocean. *Paleoceanography* 26 PA3220.
- Hintz, C.J., Chandler, G.T., Bernhard, J.M., McCorkle, D.C., Havach, S.M., Blanks, J.K., Shaw, T.J., 2004. A physicochemically constrained seawater culturing system for production of benthic foraminifera. *Limnol. Oceanogr. Meth.* 2, 160–170.
- Hodell, D.A., Curtis, J.H., Sierro, F.J., Raymo, M.E., 2001. Correlation of late Miocene to early Pliocene sequences between the Mediterranean and North Atlantic. *Paleoceanography* 16 (2), 164–178.
- Hofmann, M., Wolf-Gladrow, D.A., Takahashi, T., Sutherland, S.C., Six, K.D., Maier-Reimer, E., 2000. Stable carbon isotope distribution of particulate organic matter in the ocean: a model study. *Mar. Chem.* 72 (2–4), 131–150.

- Hönisch, B., Bickert, T., Hemming, N.G., 2008. Modern and Pleistocene boron isotope composition of the benthic foraminifer *Cibicides wuellerstorfi*. *Earth Planet. Sc. Lett.* 272 (1–2), 309–318.
- Lea, D.W., Bijma, J., Spero, H.J., Archer, D., 1999. Implications of a carbonate ion effect in shell carbon and oxygen isotopes for glacial ocean conditions. In: Fischer, G., Wefer, G. (Eds.), *Use of Proxies in Paleoclimatology: Examples from the South Atlantic*. Springer, Berlin, pp. 513–522.
- Lesniak, P.M., Sakai, H., 1989. Carbon isotope fractionation between dissolved carbonate and CO<sub>2</sub>(g) at 25 °C and 40 °C. *Earth Planet. Sc. Lett.* 95, 297–301.
- Lesniak, P.M., Zawadzki, P., 2006. Determination of carbon fractionation factor between aqueous carbonate and CO<sub>2</sub>(g) in two-direction isotope equilibration. *Chem. Geol.* 231, 203–213.
- Linke, P., Lutze, G.F., 1993. Microhabitat preferences of benthic foraminifera – a static concept or a dynamic adaptation to optimize food acquisition. *Mar. Micropaleontol.* 20 (3–4), 215–234.
- Mackensen, A., Hubberten, H.W., Bickert, T., Fischer, G., Futterer, D.K., 1993. The δ<sup>13</sup>C in benthic foraminiferal tests of *Fontbotia wuellerstorfi* (Schwager) relative to the δ<sup>13</sup>C of dissolved inorganic carbon in Southern Ocean deep-water – implications for glacial ocean circulation models. *Paleoceanography* 8 (5), 587–610.
- Mackensen, A., Rudolph, M., Kuhn, G., 2001. Late Pleistocene deep-water circulation in the subantarctic eastern Atlantic. *Global Planet. Change* 30 (3–4), 197–229.
- McCorkle, D.C., Keigwin, L.D., Corliss, B.H., Emerson, S.R., 1990. The influence of microhabitats on the carbon isotopic composition of deep-sea benthic foraminifera. *Paleoceanography* 5, 161–185.
- McCorkle, D.C., Bernhard, J.M., Hintz, C.J., Blanks, J.K., Chandler, G.T., Shaw, T.J., 2008. The carbon and oxygen stable isotopic composition of cultured benthic foraminifera. In: Austin, W.E.N., James, R.H. (Eds.), *Biogeochemical Controls on Paleoclimatological Environmental Proxies*. vol. 303. *Geol. Soc. London*, pp. 135–154.
- Michaels, A.F., Caron, D.A., Swanberg, N.R., Howse, F.A., Michaels, C.M., 1995. Planktonic sarcodines (Acantharia, Radiolaria, Foraminifera) in surface waters near Bermuda – abundance, biomass and vertical flux. *J. Plankton Res.* 17 (1), 131–163.
- Millero, F.J., 1995. Thermodynamics of the carbon dioxide system in the oceans. *Geochim. Cosmochim. Acta* 59 (4), 661–677.
- Moodley, L., Middelburg, J.J., Boschker, H.T.S., Duineveld, G.C.A., Pel, R., Herman, P.M.J., Heip, C.H.R., 2002. Bacteria and Foraminifera: key players in a short-term deep-sea benthic response to phytodetritus. *Mar. Ecol. Prog. Ser.* 236, 23–29.
- Mook, W.G., 1986. <sup>13</sup>C in atmospheric CO<sub>2</sub>. *Neth. J. Sea Res.* 20 (2–3), 211–223.
- Myrntinen, A., Becker, V., Barth, J.A.C., 2012. A review of methods used for equilibrium isotope fractionation investigations between dissolved inorganic carbon and CO<sub>2</sub>. *Earth-Sci. Rev.* 115, 192–199.
- Nomaki, H., Heinz, P., Hemleben, C., Kitazato, H., 2005. Behavior and response of deep-sea benthic foraminifera to freshly supplied organic matter: a laboratory feeding experiment in microcosm environments. *J. Foraminif. Res.* 35 (2), 103–113.
- Nomaki, H., Heinz, P., Nakatsuka, T., Shimanaga, M., Ohkouchi, N., Ogawa, N.O., Kogure, K., Ikemoto, E., Kitazato, H., 2006. Different ingestion patterns of <sup>13</sup>C-labeled bacteria and algae by deep-sea benthic foraminifera. *Mar. Ecol. Prog. Ser.* 310, 95–108.
- Nomaki, H., Yamaoka, A., Shirayama, Y., Kitazato, H., 2007. Deep-sea benthic foraminiferal respiration rates measured under laboratory conditions. *J. Foraminif. Res.* 37 (4), 281–286.
- Oliver, K.I.C., Hoogakker, B.A.A., Crowhurst, S., Henderson, G.M., Rickaby, R.E.M., Edwards, N.R., Elderfield, H., 2010. A synthesis of marine sediment core δ<sup>13</sup>C data over the last 150,000 years. *Clim. Past* 6, 645–673.
- Rae, J.W.B., Foster, G.L., Schmidt, D.N., Elliott, T., 2011. Boron isotopes and B/Ca in benthic foraminifera: proxies for the deep ocean carbonate system. *Earth Planet. Sc. Lett.* 302 (3–4), 403–413.
- Rathburn, A.E., Corliss, B.H., Tappa, K.D., Lohmann, K.C., 1996. Comparisons of the ecology and stable isotopic compositions of living (stained) benthic foraminifera from the Sulu and South China seas. *Deep-Sea Res.* 1 43, 1617–1646.
- Rathmann, S., Kuhnert, H., 2008. Carbonate ion effect on Mg/Ca, Sr/Ca and stable isotopes on the benthic foraminifera *Oridorsalis umbonatus* off Namibia. *Mar. Micropaleontol.* 66, 120–133.
- Rau, G.H., Takahashi, T., Marais, D.J.D., 1989. Latitudinal variations in plankton δ<sup>13</sup>C – implications for CO<sub>2</sub> and productivity in past oceans. *Nature* 341 (6242), 516–518.
- Sanyal, A., Hemming, N.G., Broecker, W.S., Hanson, G.N., 1997. Changes in pH in the eastern equatorial Pacific across stage 5–6 boundary based on boron isotopes in foraminifera. *Global Biogeochem. Cy.* 11 (1), 125–133.
- Sarnthein, M., Winn, K., Jung, S.J.A., Duplessy, J.C., Labeyrie, L., Erlenkeuser, H., Ganssen, G., 1994. Changes in east Atlantic deep-water circulation over the last 30,000 years: eight time slice reconstructions. *Paleoceanography* 9 (2), 209–267.
- Shackleton, N.J., 1977. Tropical rainforest history and the equatorial Pacific carbonate dissolution cycles. In: Malahoff, N.R., Andersen, A. (Eds.), *Fate of Fossil Fuel CO<sub>2</sub> in the Oceans*. Plenum Press, New York, pp. 401–427.
- Spero, H.J., Lea, D.W., 1996. Experimental determination of stable isotope variability in *Globigerina bulloides*: implications for paleoceanographic reconstructions. *Mar. Micropaleontol.* 28 (3–4), 231–246.
- Spero, H.J., Bijma, J., Lea, D.W., Bemis, B.E., 1997. Effect of seawater carbonate concentration on foraminiferal carbon and oxygen isotopes. *Nature* 390 (6659), 497–500.
- Turley, C.M., Newell, R.C., Robins, D.B., 1986. Survival strategies of two small marine ciliates and their role in regulating bacterial community structure under experimental conditions. *Mar. Ecol. Prog. Ser.* 33 (1), 59–70.
- Wilson-Finelli, A., Chandler, G.T., Spero, H.J., 1998. Stable isotope behavior in paleoceanographically important benthic foraminifera: results from microcosm culture experiments. *J. Foraminif. Res.* 28 (4), 312–320.
- Wolf-Gladrow, D.A., Bijma, J., Zeebe, R.E., 1999. Model simulation of the carbonate chemistry in the microenvironment of symbiont bearing foraminifera. *Mar. Chem.* 64 (3), 181–198.
- Woodruff, F., Savin, S.M., Douglas, R.G., 1980. Biological fractionation of oxygen and carbon isotopes by recent benthic foraminifera. *Mar. Micropaleontol.* 5 (1), 3–11.
- Zahn, R., Winn, K., Sarnthein, M., 1986. Benthic foraminiferal δ<sup>13</sup>C and accumulation rates of organic carbon: *Uvigerina peregrina* group and *Cibicides wuellerstorfi*. *Paleoceanography* 1 (1), 27–42.
- Zarriess, M., Mackensen, A., 2011. Testing the impact of seasonal phytodetritus deposition on δ<sup>13</sup>C of epibenthic foraminifer *Cibicides wuellerstorfi*: a 31,000 year high-resolution record from the northwest African continental slope. *Paleoceanography* 26 PA2202.
- Zeebe, R.E., 2007. Modeling CO<sub>2</sub> chemistry, δ<sup>13</sup>C, and oxidation of organic carbon and methane in sediment porewater: implications for paleo-proxies in benthic foraminifera. *Geochim. Cosmochim. Acta* 71 (13), 3238–3256.
- Zeebe, R.E., Bijma, J., Wolf-Gladrow, D.A., 1999. A diffusion–reaction model of carbon isotope fractionation in foraminifera. *Mar. Chem.* 64 (3), 199–227.
- Zhang, J., Quay, P.D., Wilbur, D.O., 1995. Carbon isotope fractionation during gas–water exchange and dissolution of CO<sub>2</sub>. *Geochim. Cosmochim. Acta* 59, 107–114.